In Situ Characterisation of Permanent Magnetic Quadrupoles for Focussing Proton Beams

J.J. Melone[13], K.W.D. Ledingham[123], T. McCanny[1], T. Burris-Mog[2], U. Schramm[2], R. Grötzschel[2], S. Akhmadaliev[2], D. Hanf[2], K.M. Spohr[4], M. Bussmann[2] , T. Cowan[2] , S. M. Wiggins[1], M. R. Mitchell[1]

[1] *SUPA Department of Physics, University of Strathclyde, Glasgow G4 0NG, United Kingdom*

[2] *Institut für Strahlenphysik, Forschungzentrum Dresden-Rossendorf, Bautzner Landstraße 128, 01328 Dresden, Germany*

[3] *AWE plc., Aldermaston, Reading RG7 4PR, United Kingdom*

[4] *SUPA Department of Physics, University of the West of Scotland, Paisley PA1 2BE, United Kingdom*

High intensity laser driven proton beams are at present receiving much attention. The reasons for this are many but high on the list is the potential to produce compact accelerators. However two of the limitations of this technology is that unlike conventional nuclear RF accelerators lasers produce diverging beams with an exponential energy distribution. A number of different approaches have been attempted to monochromise these beams but it has become obvious that magnetic spectrometer technology developed over many years by nuclear physicists to transport and focus proton beams could play an important role for this purpose. This paper deals with the design and characterisation of a magnetic quadrupole system which will attempt to focus and transport laser-accelerated proton beams.

I. INTRODUCTION

Outstanding progress has been made in high-power laser technology in the last 10 years with laser powers reaching petawatt (PW) values. Petawatt lasers generate electric fields of 10^{12} Vm^{-1} with a large fraction of the total pulse energy being converted to relativistic electrons with energies reaching in excess of 1 GeV. In turn these electrons can result in the generation of beams of protons, heavy ions, neutrons and high-energy photons. These laser-driven particle beams have encouraged many to think of carrying out experiments normally associated with conventional nuclear accelerators and reactors. To this end a number of introductory articles have been written under a trial name 'Laser Nuclear Physics' [1–4].

However two of the draw backs for this technology are that unlike conventional nuclear RF accelerators, lasers produce diverging ion beams with exponential energy distributions. A number of different approaches have been attempted to monochromise these beams using sophisticated shaped targetry[5], specially controlled chemical treatment of high Z metal foils[6] and the use of micro-lens technology requiring a second laser beam[7]. These approaches have had some success at the expense of increased complication.

In a recent paper entitled "What will it take for laser driven proton accelerators to be applied to tumour therapy"[8] the authors correctly pointed out that conventional nuclear magnetic transport systems could be used for transporting particles from laser accelerators with the correct energy characteristics to wherever they are needed. However they also point out that this might defeat the basic premise of compactness of the new laser technology.

On the contrary, however, over the last few years very compact permanent magnet systems using neodymium iron boron ($Nd_2Fe_{14}B$) alloy[9] sectors in a Halbach geometry[10] have been investigated as suitable magnetic spectrometers particularly with laser based systems in mind. These have been developed as miniature magnetic devices for laser based accelerators particularly to control electron beams for the production of undulator or free electron radiation[11] or inverse-Compton scattering production of X-rays[12–16]. In particular Schollmeier et al.[15] emphasise that two permanent quadrupoles (PMQ) transport and focus laser accelerated protons in a very reproducible and predictable manner decoupling the acceleration process from the beam transport allowing for independent optimisation of the processes.

The present paper will describe the design and characterisation of a Halbach system particularly designed for laser produced protons up to about 20 MeV. However for characterisation of the system protons up to 9 MeV from a tandem were used.

II. EXPERIMENTAL SET-UP

The quadrupoles employed in this experiment utilise the Halbach cylinder design as shown on the left in Fig 1. Using this configuration has the effect of increasing the magnetic flux density within the cylinder, and greatly reducing it outside[17]. This has obvious benefits for use in compact portable systems. The cylinder is constructed of 12 wedges of NdFeB alloy, where each wedge has a remanent field strength of

1.36 Tesla, and in the configuration shown in Fig 1(a), this creates a typical quadrupole field gradient of ∼110T/m. This number is mostly governed by the inner diameter of the Halbach cylinder which in this case is 25 mm. In general the quadrupoles were placed as close as possible to each other, with a small gap necessary to facilitate their separation since the attractive force between each Permanent Magnetic Quadrupole (PMQ) is intense. In the pair configuration the second PMQ was rotated at 90° with respect to the first, and this creates a standard focussing quadrupole pair configuration[18], shown in Fig 1(b).

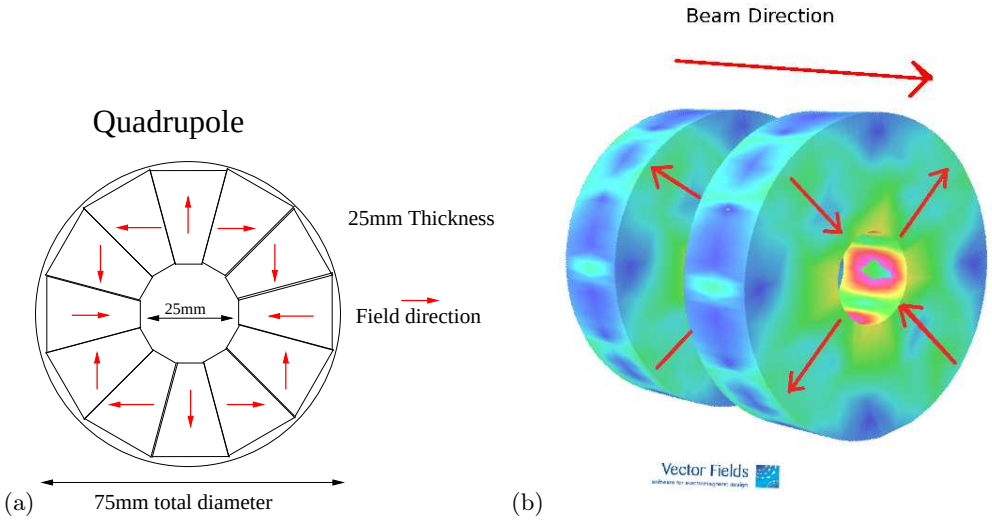

Figure 1: The Halbach Cylinder Configuration(a) and the quadrupole focussing pair(b).

Since this experiment describes the characterisation of this quadrupole pair, a test-bed was constructed to allow the accurate placement of the PMQs within a beam-line, and also to create fixed measurement points for the detection system. Fig 2 shows a vacuum-tight steel tube which is designed to house the PMQs and various holders and spacers which regulate the distances and hold the Halbach cylinder PMQ in place. This tube is attached to the Forschungzentrum Dresden-Rossendorf Tandem Accelerator beam-line[19] which can produce protons beams of energy up to 9 MeV.

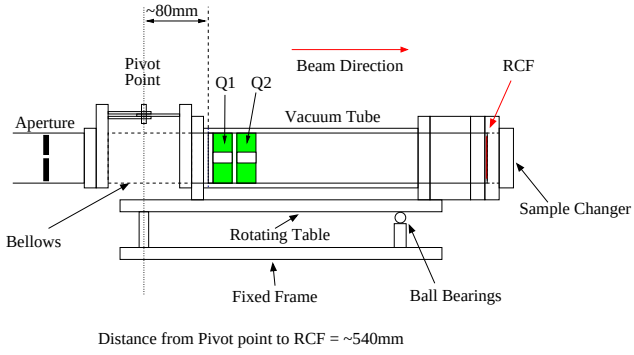

Figure 2: The overall set-up with magnets and radio-chromic film (RCF).

The design incorporates a custom-built flange which places pieces of radio-chromic film (RCF) at a specific distance downstream from the PMQs (See Fig 2 for Sample Changer), and the supporting structure for the vacuum tube allows for movement of the tube with reference to a pivot point 8.5cm upstream from the end of the tube. This has the effect of replicating the situation where particles are transported into the PMQs with a specific angle of incidence, and one of the main results measured shows the effect of varying angles of incidence on the properties of transport and focussing that the PMQs demonstrate.

III. METHOD

The experimental run at FZD was carried out using the Tandem accelerator which produced proton energies of up to 9 MeV, at a typical beam current of 1-10 picoamperes. This beam was tested, first without PMQs in position to check the transport and alignment of the beam through the system, then with one PMQ only, then with two PMQs arranged as a focussing pair. The beam was passed through an aperture upstream of the pivot point and tube, which regulated the beam spot-size. The PMQ pair was typically placed at a distance of 25 mm apart which then defines the strongest part of the field created by each PMQ as being 50 mm apart. This reduced the extent to which the fields from a pair of PMQs interacted and made them far easier to handle.

A. Focal point analysis

For the first part of the run a 1mm beam aperture was used, however alignment issues forced the adoption of a 2mm aperture for later runs. Once a suitable centre-point position for the moveable table supporting the system was established, the aim was to fire the proton beam through the PMQs in unchanging conditions, varying only the angle of incidence, achieved by moving the support table a set distance from the centre-position, in intervals corresponding to 1 degree. From this process, the effect of the PMQs on incident 9 MeV proton beams with 2mm diameter and varying angle of incidence could be recorded on a single piece of RCF. To analyse the effect of the PMQ pair on the pencil beam produced by the accelerator, the configuration in Fig 2 was used and the incident angle was varied between 0-4 degrees, producing an array of spots on the RCF which are discussed later.

B. Definition of magnet focussing power and focal length

For the case of a charged particle travelling with speed v perpendicular to a magnetic field B, the force experienced by the particle is $F = qvB$. The resulting circular trajectory has a radius $\rho = \frac{mv}{qB}$, varying proportionally with the particle's charge, momentum and the strength of the external magnetic field. For a proton charge of $q = +1$, $B\rho = mv$. The field gradient is defined as $K = \frac{dB_y}{dx}(Tm^{-1})$, where the x-y plane is in the plane of the B-field. A quantity taking account of the incident particle momentum and charge is the normalised field gradient defined as $k = \frac{K}{B\rho}$, and this is also known as the focussing strength of the quadrupole[20]. For a quadrupole where the region of the B-field has a length L, the normalised field gradient applies over this distance to give a focussing power of $\frac{1}{f} = \frac{KL}{B\rho}$, hence the focal length is $f = \frac{B\rho}{KL}$, or in terms of the focussing strength, $f = \frac{1}{kL}$. The PMQs shown in Fig 1 have a measured field gradient of $100Tm^{-1}$, which for 9 MeV protons gives a normalised field gradient of $k = 268.5$, and a focal length $f = \frac{1}{0.025*k} = 0.15m$.

The focal length of 15 cm for this field gradient agrees closely with proton trajectory calculations made in TOSCA[21] (See Fig 3). This calculation shows only the focussing effect in the x-plane, and there is an equal de-focussing effect in the y-plane for a single PMQ. Using a combination of similar PMQs in the FODO (focussing-zero-defocussing-zero) configuration gives an overall focussing effect, as long as the separation distance between the pair is less than the focal length of a single PMQ. If each PMQ was infinitely thin, a single focal point would be the end product of such a PMQ pair. In reality a finite dimension PMQ pair where the first PMQ focusses in the X-direction will produce a focal line firstly in X, then a similar orthogonal focal line in Y some distance downstream.

It is also possible to use a quadrupole triplet with a focussing-defocussing-focussing effect (ABA configuration), which will constrain the diverging beam in 1 dimension and tightly focus it in the other. There is a larger amount of focussing overall in this arrangement than the traditional PMQ pair, which makes this configuration worthy of further investigation.

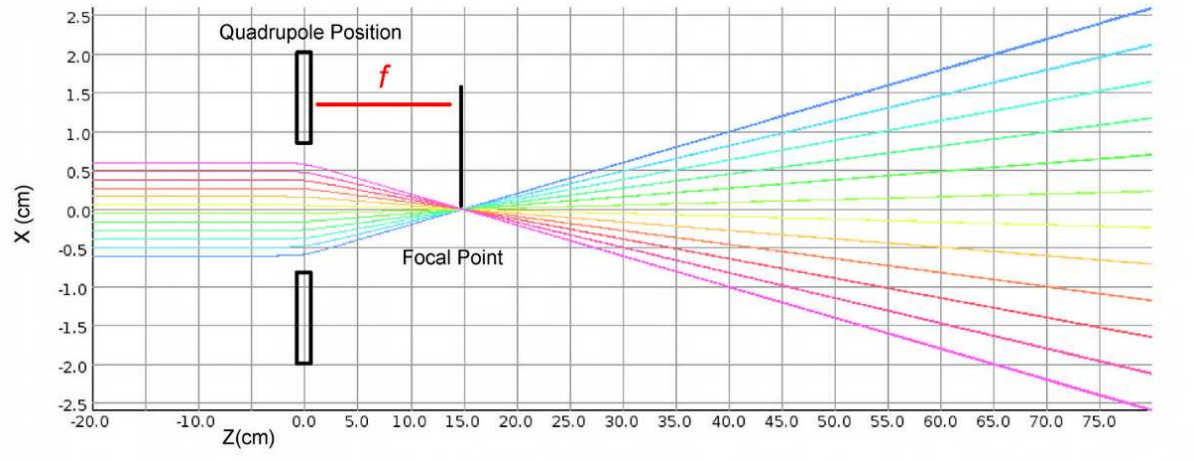

Figure 3: TOSCA calculation of 9 MeV proton trajectory through a typical single PMQ magnetic field.

C. Pencil beam ellipse analysis

A useful way of characterising the PMQ pair is to look at the elliptical distribution which defines the distortion of a circular acceptance angle. This should be reproducible if the experimental set-up is accurate, although a significant challenge arises from the fact that the support table for the set-up can only move in one plane. One solution to this is to rotate the PMQ pair through 45° and 90° from the original position, and if the RCF is also rotated, this should be consistent with the conditions producing the typical ellipse. A modification of the setup used in Fig 2 is used to ensure the placement of the PMQ pair is fixed with respect to the RCF, seen in Fig 4. This arrangement is more suitable for the purpose of measuring the elliptical acceptance of the PMQ pair, as the RCF position and angle were fixed relative to the PMQ orientation, which allows the results to be treated as if the incident beam can travel at any angle deviating from the beam-line rather than being limited to the horizontal plane, and greatly eases the analysis of the RCF.

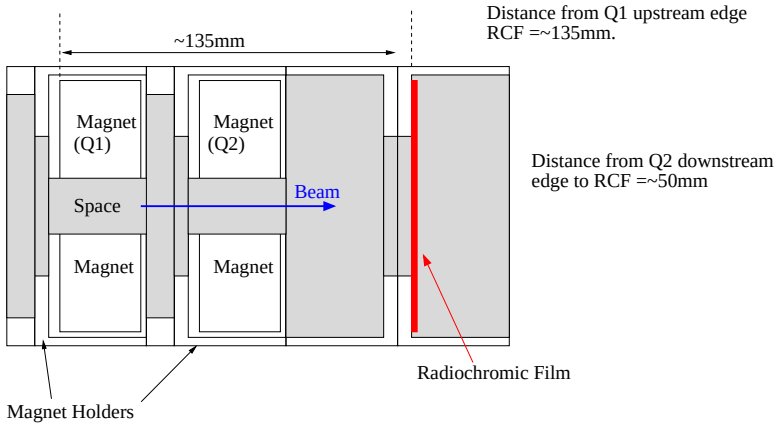

Figure 4: Shortened setup for analysing the typical ellipse produced by the PMQ pair.

D. Scattered divergent beam analysis

Another method of characterising the quadrupole pair is to look at the effect of the magnetic field on a divergent incident beam. The method for this approach is to use a scattering foil upstream and close to the first quadrupole, as shown in Fig 5. A comparison is then possible between the original scatter distribution, with characteristic energy distribution and divergence determined by the thickness and material of the radiator used as the scattering foil, and the case where the quadrupole pair alter the trajectories of the protons.

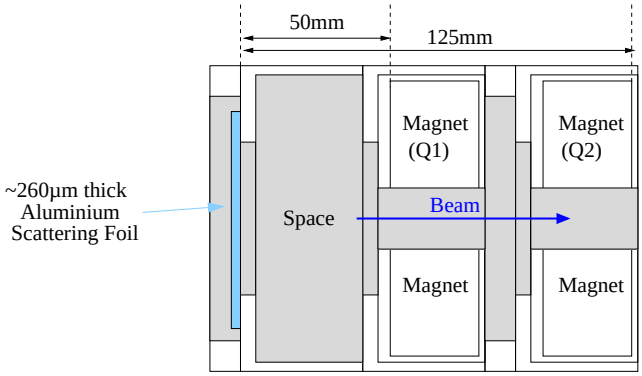

Figure 5: Shortened setup for analysing the effect of the PMQ on a divergent beam produced by a scattering foil.

E. Scattered divergent Beam with pepperpot beamlet analysis

From limitations inherent in the experimental design, it follows that better control over the incident angle is necessary for proper replication of the results using this type of experimental set-up. A static method, for generating several protons beams at once with varying incident angles but equivalent experimental conditions passing into the test-bed system, would give many experimental observables that would characterise the PMQ pair and also greatly reduce the time spent on changing the settings of the experiment. One way of meeting these goals is to use a "pepperpot", which is a foil or plate with many small holes passing through it. The other component of this method is to use a scattering foil as described in the Scattering Divergent beam analysis section. If the holes are machined accurately, it is possible to deduce the incident angles of any set of beams passing though the pepperpot from a point-like source incident on the scattering foil if the distance between the scattering foil and pepperpot is known.

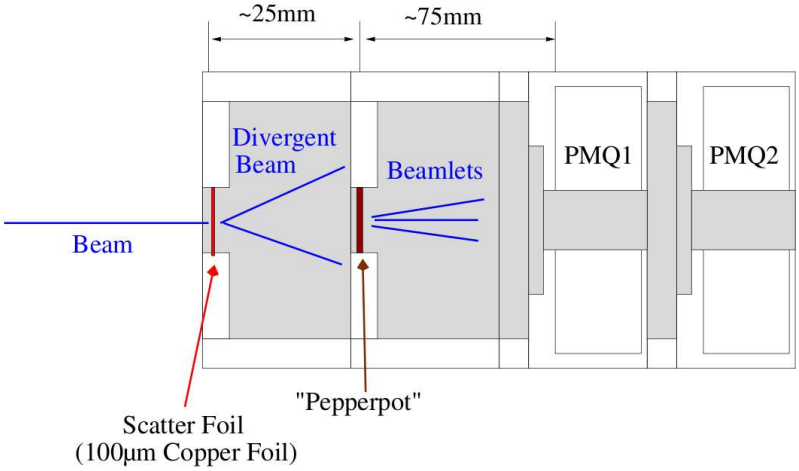

Figure 6: Simulated "Pepperpot" set-up. An aluminium scattering foil was simulated, with a thickness of 130µm.

Fig 6 shows the setup used at FZD during the experiment. The pepperpot had a grid consisting of 121 holes of radius 50µm and with a pitch of 1.25mm. This pepperpot was created by using a micro-machining technique utilising high-power femtosecond lasers to machine metal foil samples[22].

Laser pulses of 800nm wavelength and 40 femtosecond pulse duration are typically applied at a repetition rate of 1 kHz, with an energy per pulse of 0.06 mJ, to drill holes via the laser ablation process on a metal foil[23]. The machined holes are approximately circular and have a diameter proportional to the laser focal point diameter. The process is easily automated for the production of grids and structures. Fig 7 shows an example of the quality and dimensions of holes produced in 250µm thick tungsten foil very similar to the one used in the experiment, using the Femtosecond laser system of the TOPS facility at University of Strathclyde.

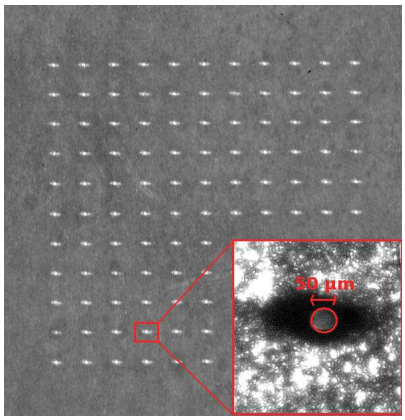

Figure 7: Example of Femtosecond Laser micro-machining produced at University of Strathclyde with the TOPS laser system. The grid above consists of 11x11 holes at a pitch of 0.5mm and 50µm diameter.

The set-up as described in Fig 2 must be modified slightly as shown in Fig 8 to accomodate the pepperpot, and to allow space for the placement of RCF segments to record the beamlet positions and intensities. The pivot and bellows are removed in this set-up since they were unneccesary. A small 0.5mm radius aperture was used, and the scatter foil was placed immediately downstream, with the rest of the geometry the same as Fig 6. A third quadrupole can be optionally added to this set-up, and the results of the triplet of quadrupoles placed in an A-B-A configuration (where B is orthogonal to A around the z-axis), are discussed in the analysis section below.

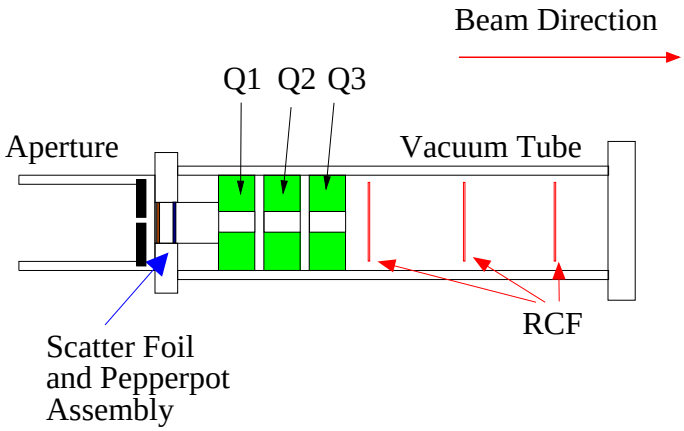

Figure 8: The modified experimental set-up used to implement the pepperpot. RCF segments were placed at intervals along the length of the vacuum tube to capture the evolving profile of the beamlets and their spatial distribution.

F. Selection of Scattering Foil and Pepperpot positions

As demonstrated above, the focal length of an ion lens such as a quadrupole magnet depends on the incident particle energy as well as the magnetic field strength. Given the variety of possible usage of a system of quadrupoles, it was decided to allow ample space between the scatter foil, pepper pot and the quadrupoles. Trial and error allowed the refinement of the placement of the pepperpot, since when placed closer to the magnets, more of the beamlets pass through the system, and the reverse happens when the pepperpot is placed closer to the scatter foil. So the system can be optimised for the desired running conditions. For the 9 MeV proton beam, which equates to a 6 MeV divergent beam traversing the system after passing through the 100µm copper scatter foil shown in Fig 6, placing the pepperpot 75mm downstream from the scatter foil allowed all of the beamlets through, and placing the pepperpot 25mm from the scatter foil greatly reduces the acceptance of the beamlets through the system. Fig 9 shows a simulation of this from GEANT4.

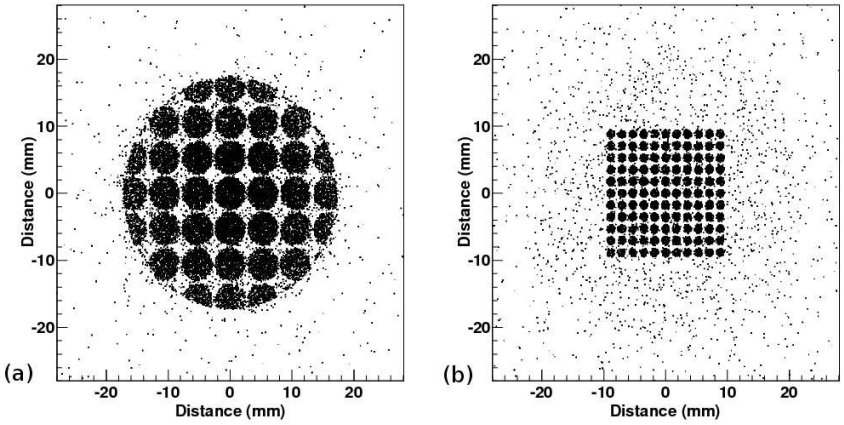

Figure 9: Figure 9(a) demonstrates that a setup with the pepperpot closer to the scatter foil produces clipping of the beamlets. Figure 9(b) shows that a setup with the pepperpot further from the scatter foil allows them all to pass through.

The angular resolution and acceptance of each beamlet changes as the distance between the scatter foil and Pepperpot changes. For the configuration in Fig 9(a), each beamlet has an increased divergence angle of $1.14(\pm 0.11)^\circ$, while for the configuration in Fig 9(b), the increase in divergence angle for each hole in the pepperpot is $0.38(\pm 0.04)^\circ$. From this it is possible to estimate the acceptance of the magnet system (limited by the inner bore of the PMQs when in the pair configuration) when the source is at a distance of 10cm as being approximately 3°.

IV. EXPERIMENTAL DATA AND COMPARISON WITH SIMULATION

The results obtained are directly visible blue spots on RCF, of type GAFCHROMIC HD-810. The intensity of the blue colour is proportional to the radiation dose received, and for the scattering results below the RCF was scanned to get an estimate of the radiation intensity. The comparison with simulation is done using the CERN physics simulation package GEANT4[24]. A simulated field-map of the Halbach cylinder design has been produced using TOSCA[21], a magneto-static scalar-field problem-solving package. This field-map contains the magnetic field components at each point in space throughout the design, even outside the magnets themselves, and GEANT4 can then track charged particles through the field, using well-known stepping algorithms such as the Runge-Kutta method[25]. Comparison with the RCF results is then achieved by using an equivalent geometry to the real-world setup (see Fig 10), and analysing the predicted proton distribution at a given distance downstream from the PMQs which corresponds with the actual positions used for the RCF.

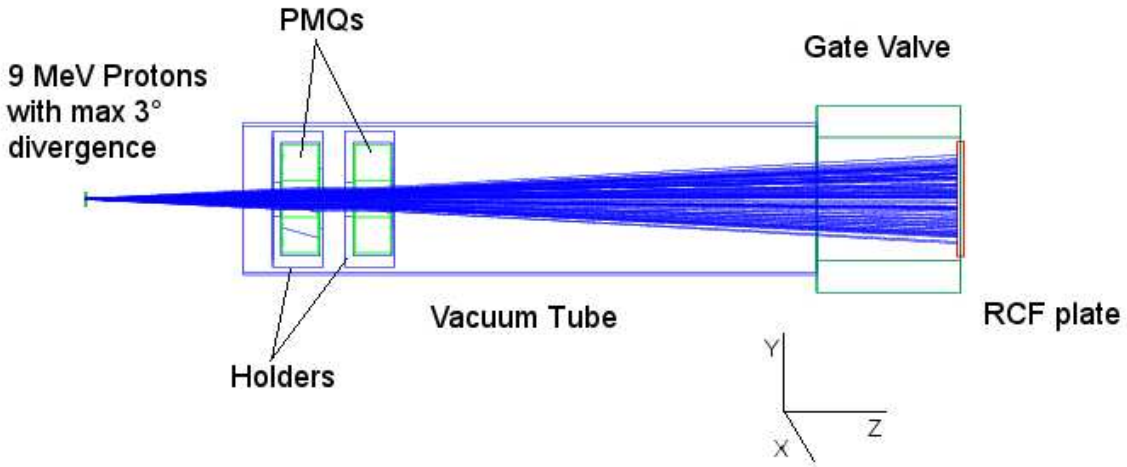

Figure 10: The GEANT4 simulation geometry. Dimensions exactly corresponding to the experimental setup are shown above, with a 9 MeV proton beam with 3° opening angle displayed passing through the system with the simulated magnetic field present. The relative orientation of the system with respect to X,Y and Z axes in the simulation is displayed.

A. Focal point results and comparisons

In Fig 11 below, the results of firing the accelerator proton beam at 9 MeV with a current of 1-10 picoamperes for a duration of 15s per measurement are visible as blue ellipses. As explained in the method we measured at a range of incident angles, and this is shown in Figs 11 and 12, where measurements from 0-4° are clearly shown.

The simulation results are also shown in Fig 11, and the sizes and positions of the focal points obtained through the PMQ pair, are comparable in size and position, suggesting that the main source of experimental error here may be the positioning of the rotating table.

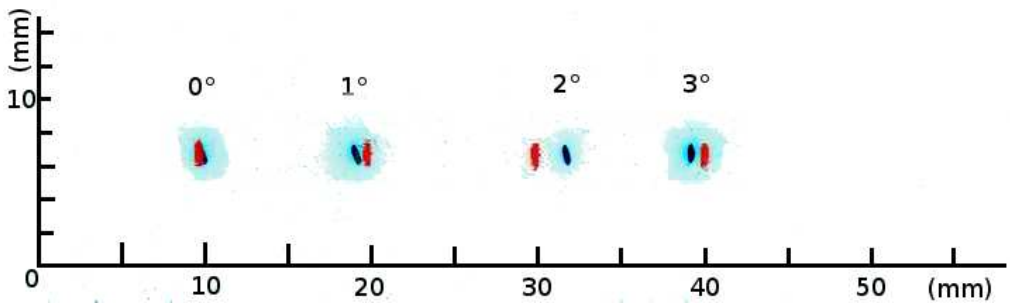

Figure 11: The RCF data is blue, and the GEANT4 prediction is red. The separation between red and blue is a measure of angular accuracy. In this and all other plots showing position and scale, the placement of the point at 0° is arbitrary, so the positions given are relative only.

B. Pencil beam ellipse results and comparisons

For analysing the elliptical acceptance of the PMQ pair, and looking at the consistency and quality of the focussing, measuring the resulting position and shape of the pencil beam gives useful data, and in Fig 12 the RCF shows the result of using the configuration discussed in the method. The variation in distance between 1° and 2° is present even when the PMQ-RCF assembly of Fig 4 is rotated, indicating a systematic error in the angular position. There is clearly a much-increased angular acceptance in the x-plane in Fig 12, where protons with up to 4° incident angle will still pass through the PMQ pair, and in the y-plane, only 2° or lesser incident angle protons will pass through. This is the expected behaviour

of the PMQ pair, since charged particles will typically be focussed in one plane first, then the orthogonal plane second. Also, while focussing in one plane, a single PMQ disperses in the orthogonal plane, and this effect dictates the acceptance of the pair, along with position, particle e/m and kinetic energy.

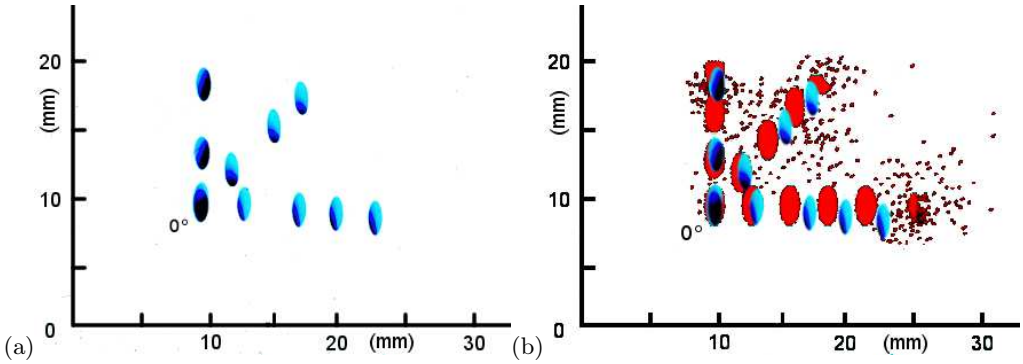

Figure 12: Result of using the setup described in Fig 4 and rotating the assembly through 2 steps of 45° each, and varying the incident angle between 0° and 4°. The experimental data is shown in (a) and the GEANT4 simulation is overlaid for comparison in (b)

The results in Fig 12 show that the angular acceptance is indeed elliptical, and the GEANT4 prediction agrees with the general shape and size of each ellipse. The increased size of each ellipse relative to the results in Fig 11 is due to the fact that the RCF is much closer to the PMQ pair than in the original beamline setup, which is further evidence of the focussing effect of the PMQ pair on a pencil beam.

GEANT4 predicts a more regular distribution, and two factors seem to cause some distortion in the data. First, the angle of incidence is underestimated in the experiment compared with the simulation where these angles are known exactly. GEANT4 predicts almost 5° angular acceptance in the x-plane which isn't corroborated by the data. One straightforward explanation for this is the increased angular step between 1° and 2° seen in the data due to inaccuracies in obtaining the desired angle.

Second, there is also some evidence of an uneven distribution within the beam spots themselves which could be due to: multiple scattering effects arising from the beam passing through the aperture, or possibly beam focussing and steering problems upstream from the test-bed location. The consistency of this effect within the beam spots would seem to indicate that this is a systematic effect characteristic of the experimental set-up, and more work is required to investigate if this is reproducible with similar beam parameters. The slight deviation in the x-plane is due to the fact that the proton beam was not travelling exactly through the centre of the magnets, and the effect on the position is more pronounced at larger incident angles.

C. Scattered divergent beam results and comparisons

Using the configuration shown in Fig 5 the results in Fig 13 were obtained from a piece of RCF placed at 400mm from the scattering foil. The mean proton energy passing through the system when using a 260µm aluminium scattering foil is calculated from GEANT4 to be ∼4.75 MeV. The experimental setup was not identical in both cases here since the unfocussed data do not have the magnets present so the angular acceptance is not limited by their inner diameter. However a comparison is still possible by establishing the blue intensity through the central area of both plots. This is done in both the X and Y planes by analysing the average blue intensity over a user-selected line through the RCF to be analysed.

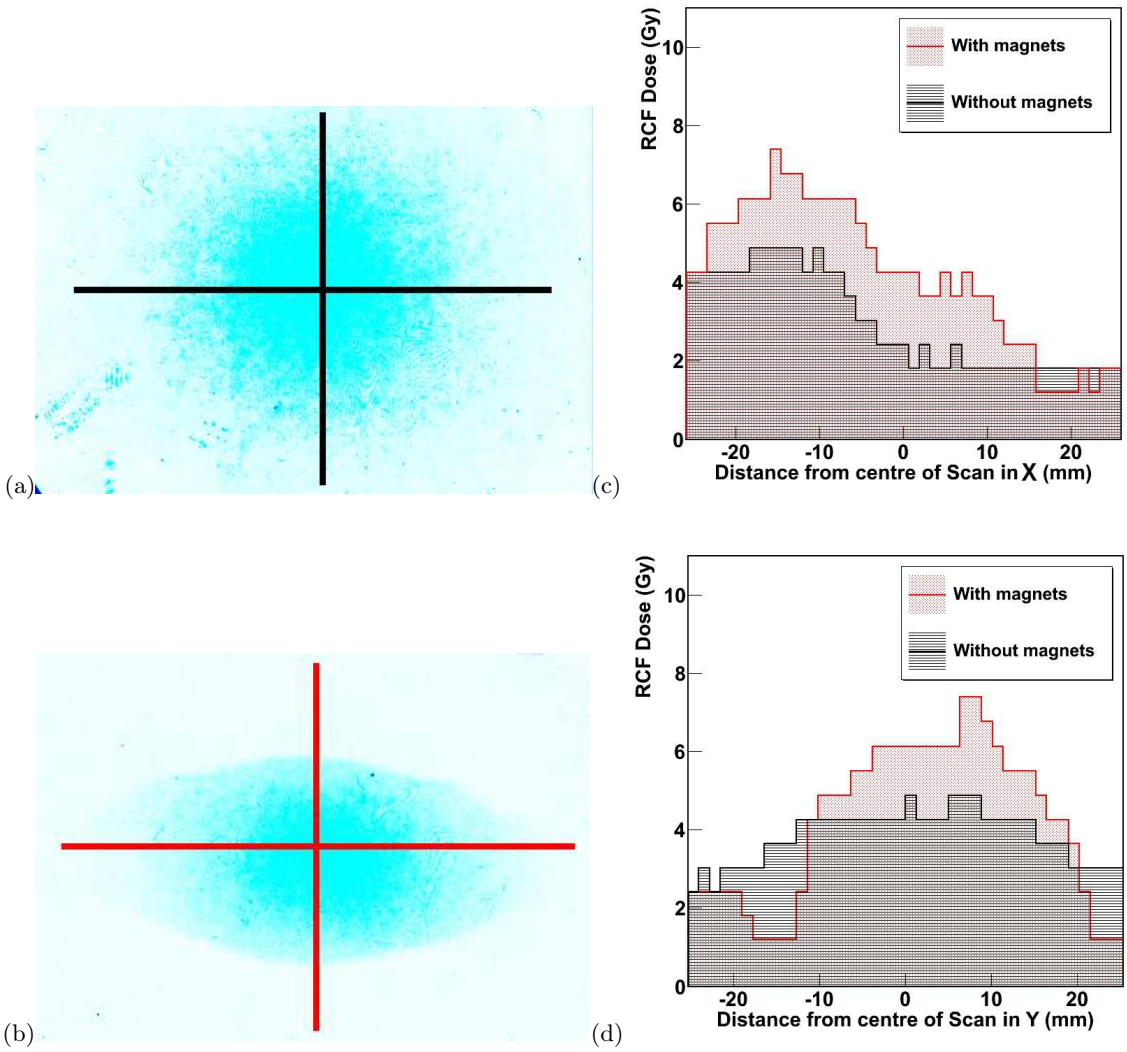

Figure 13: On the left, the RCF data showing the lines used for the profile analysis; (a) unfocussed (b) focussed. On the right (c) the profile analysis from both runs on the horizontal (X) plane, and (d) the vertical (Y) plane. The distance offset from zero in (c) is due to limitations in the area of RCF that the scanner could scan.

Although the acceptance difference between the two RCFs is obvious, an analysis of the radiation dose of the central region of both RCFs show a clear increase in dose in when the PMQ pair is present. Despite the statistical errors due to low numbers of protons available for analysis, the relative increase in yield from introducing the PMQs into this divergent beam is estimated to be ~25-35%.

The data shown in Fig 13 was analysed using an adapted MATLAB routine[26] which uses a dose calibration curve for the red, green and blue pixel values of a scanned RCF image. This routine was modified to run in ROOT[27], and was used to generate a profile analysis of the radiation dose measured by the RCF. The distance offsets seen in the profile analyses are due to physical offsets from the centre of the RCF image introduced when scanning the data. The scanner used is a Nikon Super COOLSCAN 9000 ED.

A GEANT4 simulation of this setup was also carried out, using 10^5 protons with 9 MeV initial energy passing through a scattering foil of 260µm thick aluminium . Fig 14 shows the effects of the simulated PMQ pair on the scattered proton beam, and there is a clear agreement in the shape and intensity of the focussed ellipse with the experimental data shown in Fig 13, and this is also evident when the angular distribution of protons is analysed at the RCF position in the simulation. A similar increase in proton yield , with maximum enhancement at the beamline centre, is seen in both X and Y planes, which indicates that the behaviour of the simulated magnets is in agreement with the real PMQ pair.

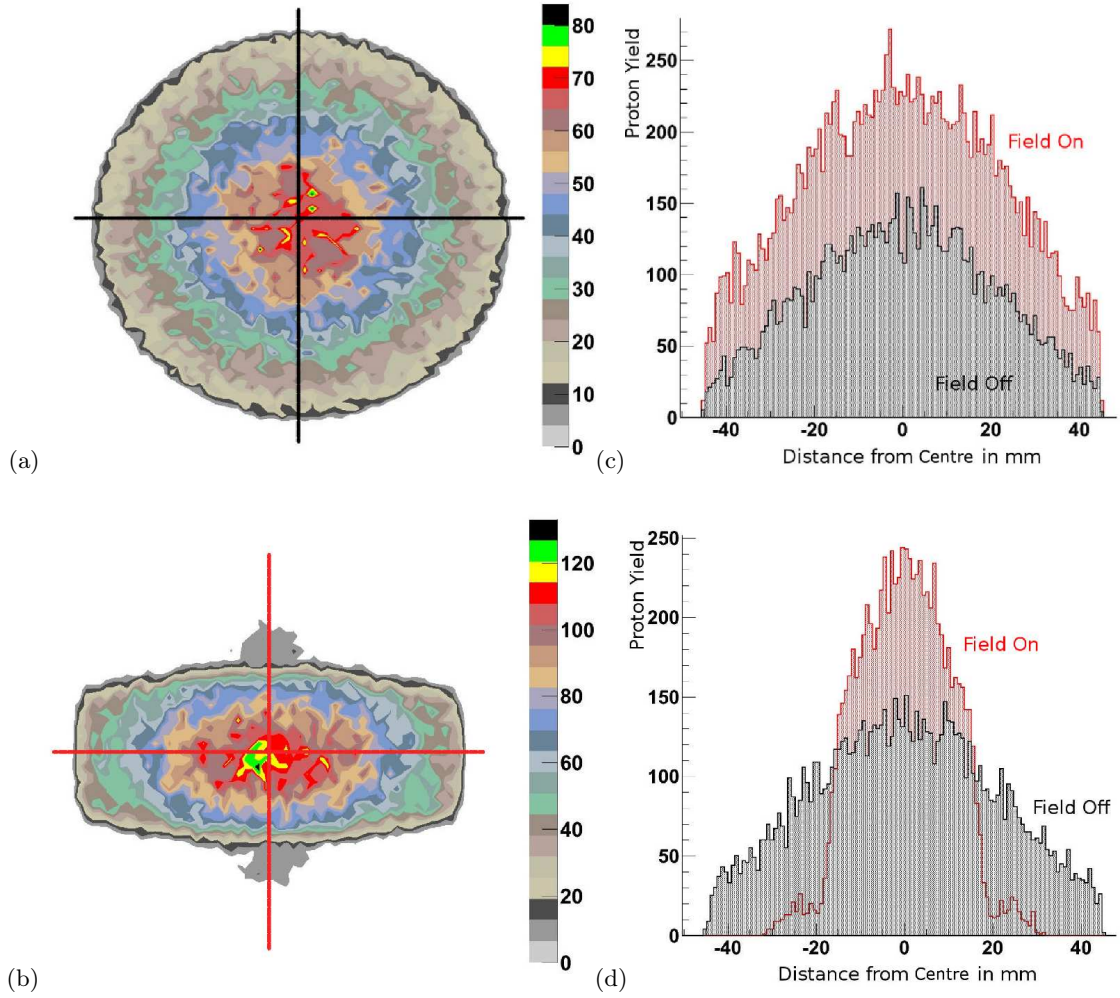

Figure 14: The GEANT4 simulation of the scattering beam setup. On the left, the angular distribution at the RCF position (a) unfocussed (b) focussed. On the right (c) a profile analysis in the horizontal (X) plane, and (d) the vertical (Y) plane.

D. Pepperpot results and comparisons

The original divergent proton beam produced by the scattering foil reduces the tandem-provided 9 MeV down to an average energy of 5.97 ± 0.19 MeV. The beam is still very forward-peaked and has an opening angle of ∼14 degrees, with both parameters measured in GEANT4. A run using 7.5 MeV from the tandem was also used and this provided a beam with an average proton energy of 3.79 ± 0.22 MeV and an opening angle of ∼ 16 degrees. The data produced by the pepperpot and scattering foil on a single RCF sheet placed at 400mm behind the scattering foil, with no magnets present, can be seen in Fig 15, where the gradient in Fig 15(c) is due to a mis-alignment of the pepperpot about the beam axis, with an angle of ∼20 degrees. Also clearly visible is an overlap between the beamlets in the X-direction (See Fig 15(b)), which almost doubles the dose in these areas. This is not a direct focussing effect from the PMQs, in fact it is due to the geometry of the pepperpot which dramatically reduces the proton intensity at the RCF, so the effect may be considered as a systematic error in the method.

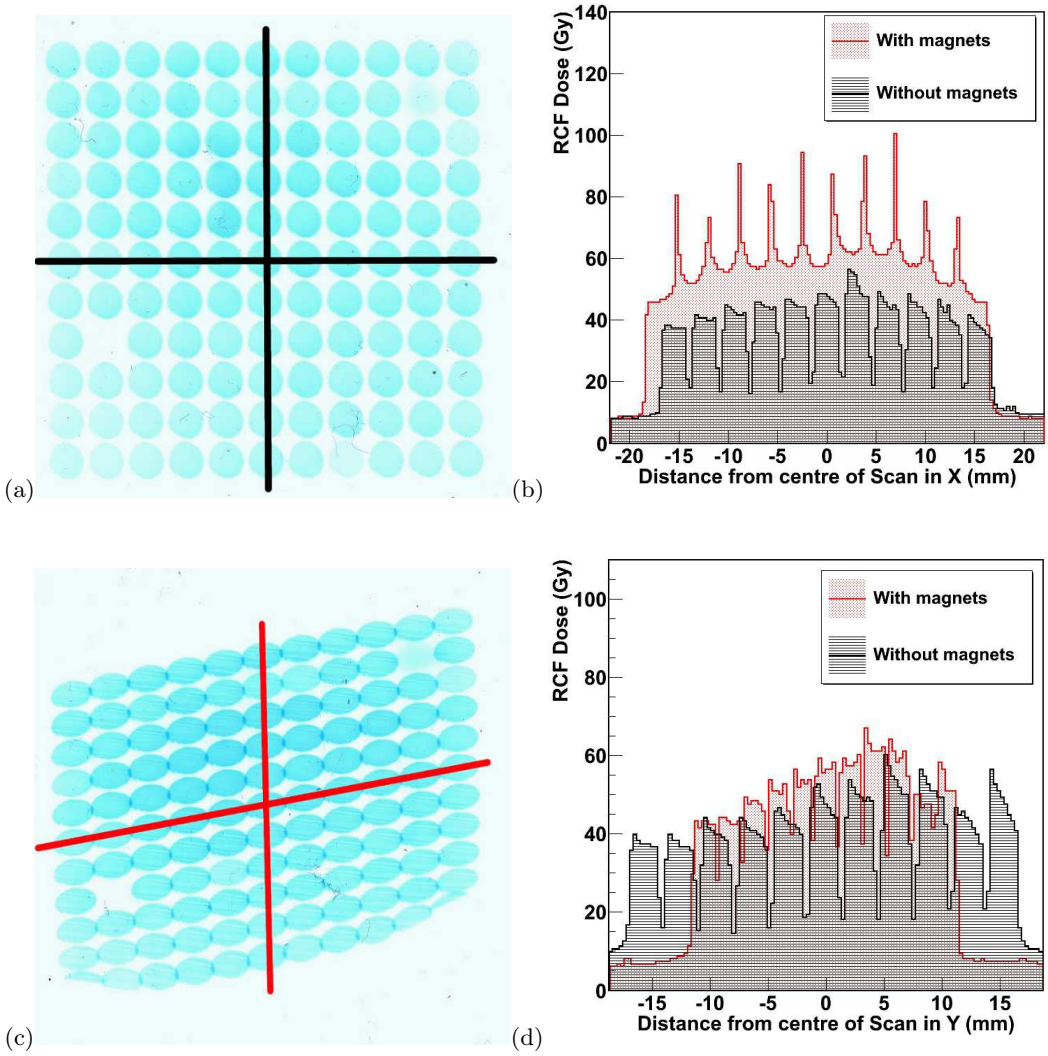

Figure 15: Pepperpot results on RCF 400mm downstream from scattering foil using a 9 MeV tandem proton beam. On the left (a) shows the results with no PMQs present, (c) shows the results with the PMQs present, and on the right (b) shows a horizontal profile analysis comparing (a) and (c), (d) shows the profile analysis performed in the vertical direction. . The lines indicate the positions where the RCF was analysed.

A GEANT4 simulation of 2×10^8 protons was carried out using the same experimental parameters and the field-map produced by TOSCA. The equivalent data and analysis are shown in Fig 16. It is clear that the focussing and enhancement in intensity is less here than in Fig 13, due to the higher proton energy.

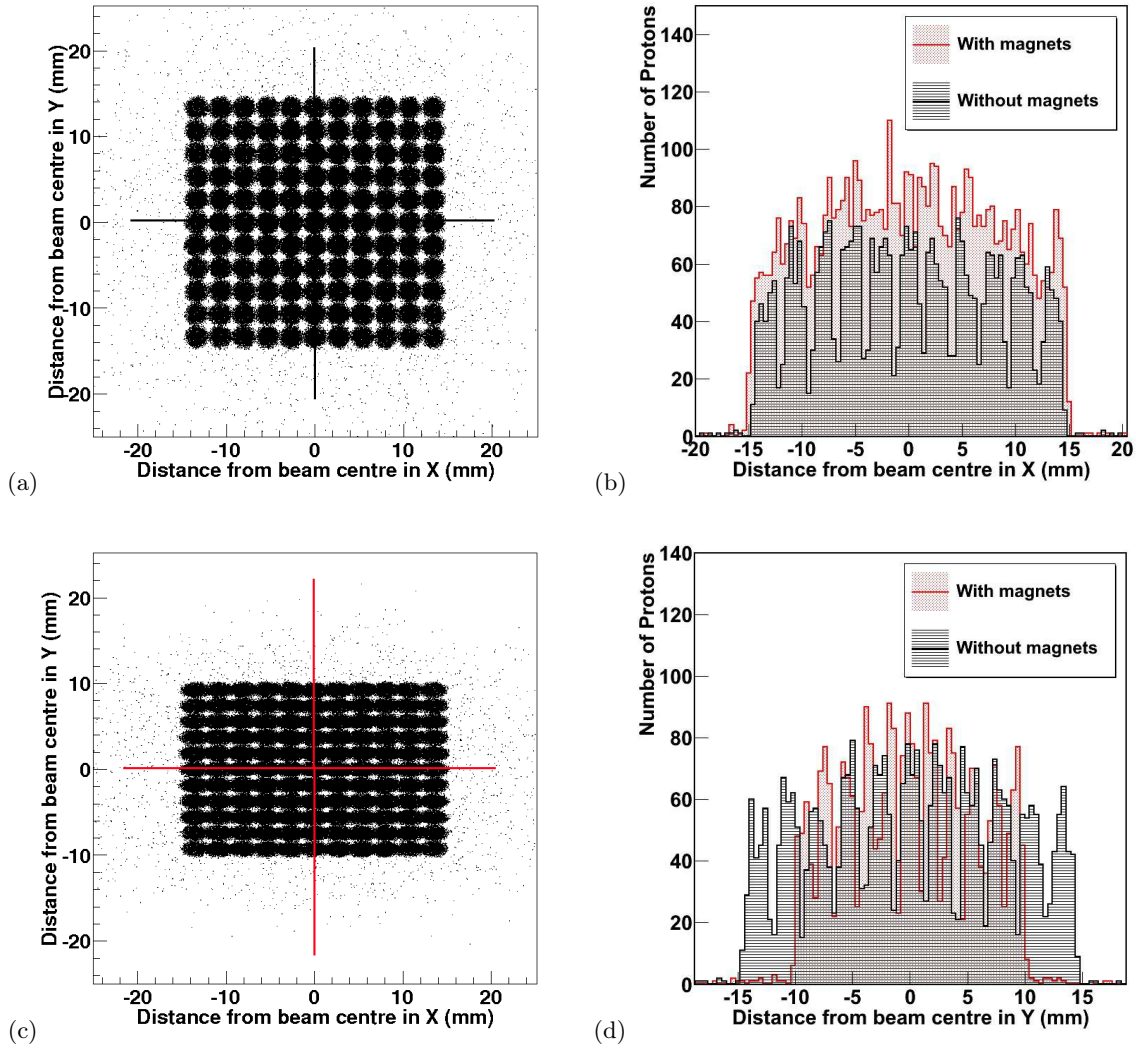

Figure 16: The GEANT4 simulation of the Pepperpot setup on RCF 400mm downstream from scattering foil. On the left (a) shows the results with no PMQs present, (c) shows the results with the PMQs present. On the right (b) shows a horizontal profile analysis comparing (a) and (c), (d) shows the same analysis performed in the vertical direction.The lines indicate the positions where the RCF was analysed.

E. Transport Properties for Diverging beam

As a measure of the transport qualities of the beam, a number of RCF segments were used at known distances downstream of the PMQs to allow study of the evolution of the beam distribution as a function of distance. Firstly, a quadrupole pair was used with a tandem proton beam energy of 7.5 MeV. Four segments of RCF were used in the vacuum tube to obtain a profile of the beam downstream of the magnets, and the results of this are shown in Fig 17(a). The simulation results from GEANT4 are compared with the results in Fig 17(b), and the main features of the data are reproduced. In terms of angular distribution and acceptance angle of the incident beam, the simulations match what was measured during the experiment.

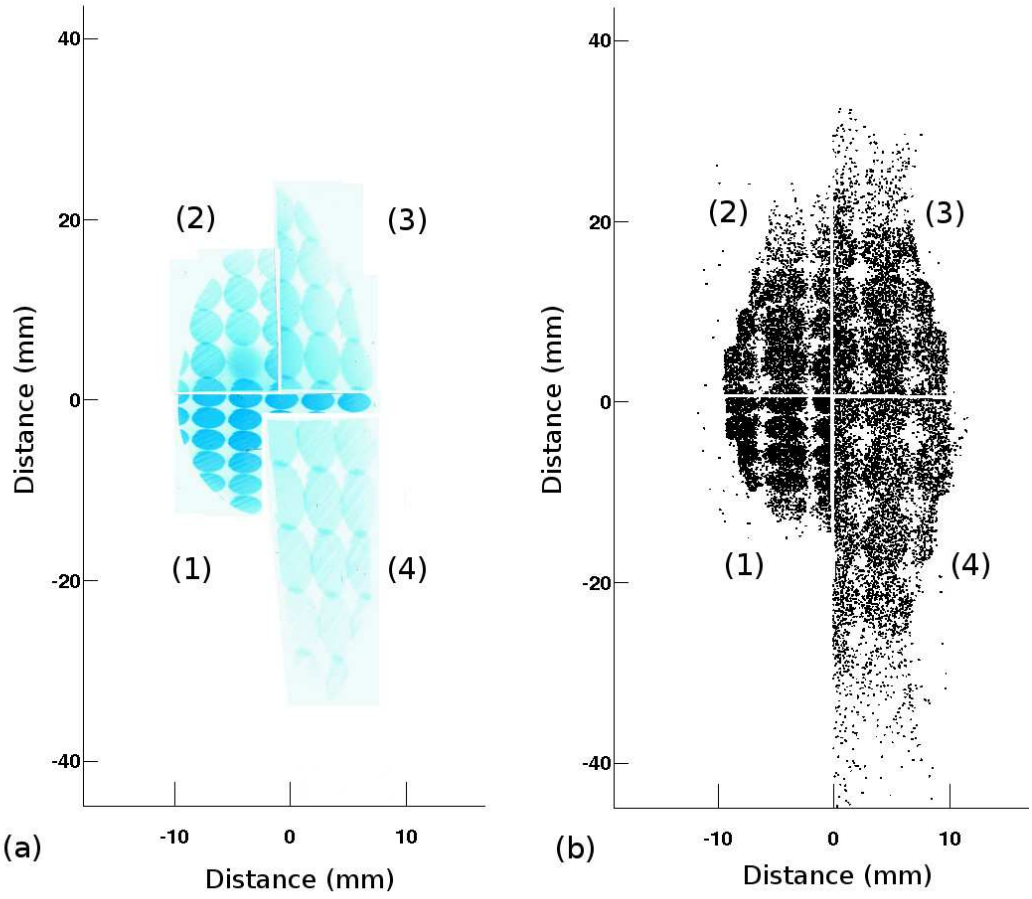

Figure 17: (a) Transport of the beam through 2 quadrupoles at 7.5 MeV using four RCF segments placed at 200mm(1), 276mm(2), 352mm(3) and 442mm(4) from the scatter foil. (b) Matching GEANT4 simulation run using $2x10^7$ 7.5 MeV protons and matching RCF positions.

F. Quadrupole triplet focussing

Using a triplet of quadrupoles in A-B-A configuration, where B is an equivalent quadrupole to A rotated through 90° around the beamline direction, gives a distinct focus point in one plane (the plane of the focussing direction of both "A" magnets). Such a system can transport a proton beam with very little dispersion in the focussing plane, with the caveat that a larger deegree of dispersion will occur in the defocussing plane. In this experiment, a different set-up (See Fig 8) was used with sections of RCF placed at intervals downstream from the magnet system. It is clear in Fig 18 that the triplet system has highly constrained a divergent beam with 14° opening angle and 5.9 ± 0.2 MeV energy in the focussing plane. This effect is even stronger when the beam energy is 3.8 ± 0.2 MeV with a slightly different opening angle of 16°, as can be seen in Fig 19.

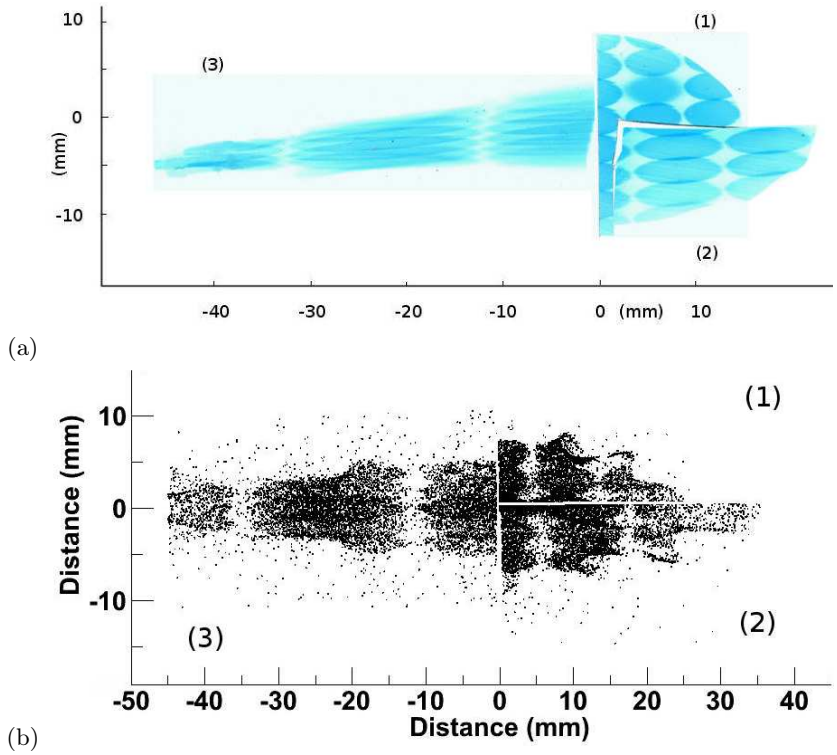

Figure 18: (a) Transport of the beam at 9 MeV using three RCF segments placed at 296mm(1), 372mm(2) , and 620mm(3) from the scatter foil. (b) Matching GEANT4 simulation run using 2x10^7 9 MeV protons and matching RCF positions.

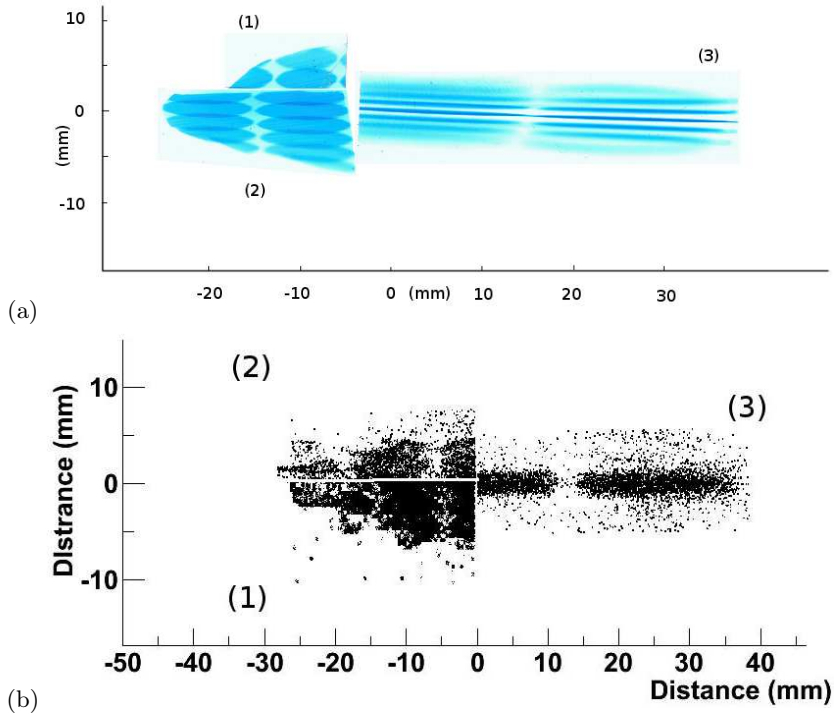

Figure 19: (a) Transport of the beam through 3 quadrupoles at 7.5 MeV using three RCF segments placed at 296mm(1), 372mm(2) , and 620mm(3) from the scatter foil. (b) Matching GEANT4 simulation run using 2x10^7 MeV protons and matching RCF positions.

A comparison of the beam distribution at 442mm from the scatter foil without the PMQ triplet, and at 620mm with the triplet in place, as shown in Fig 20, shows very clearly that Halbach design PMQs

can dramatically shape and intensify divergent particle beams, and therefore should be extremely useful in many forthcoming applications of high power laser acceleration technology.

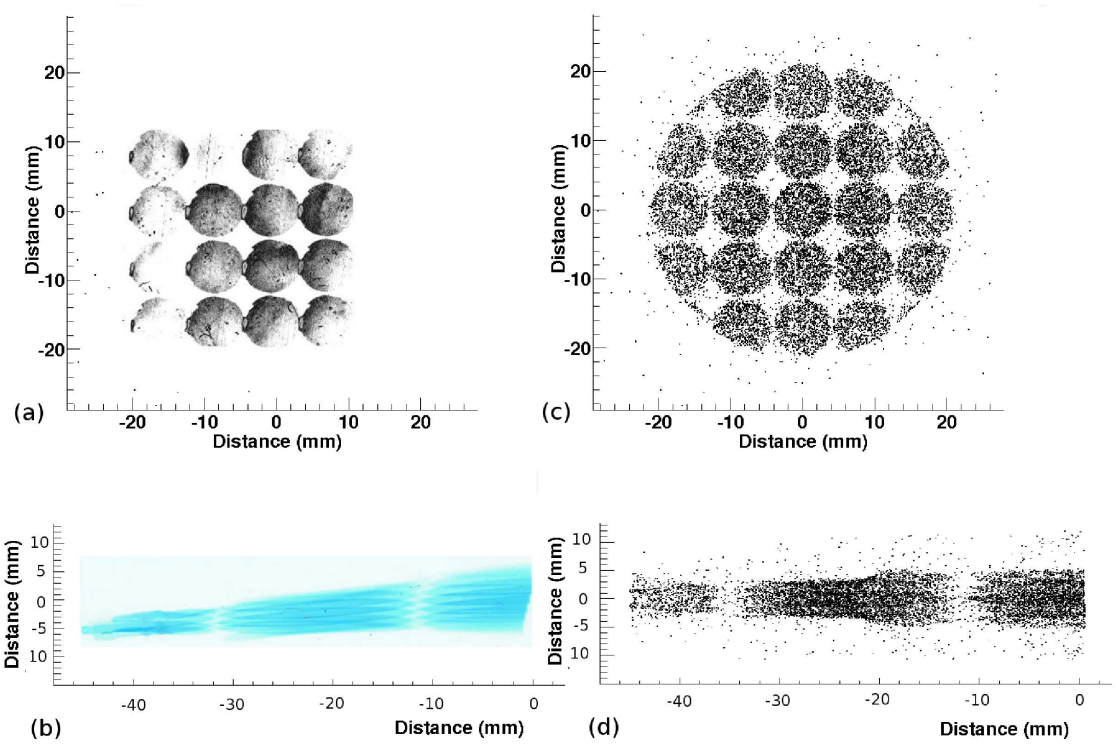

Figure 20: A comparison of RCF results with no magnets present at 442mm from the scatter foil(a), and with the PMQ triplet present at 620mm from the scatter foil(b). This is reproducible with GEANT4 (see (c) and (d)).

An analysis of the PMQ triplet RCF data shown in Fig 20 was carried out using the calibrated dose routine in ROOT, with the results shown in Fig 21. The increase in intensity seen on the RCF film using the PMQ triplet rises as high as 400% at peak. Allowing for the fact that the data with no PMQ triplet present was taken closer to the scatter foil by 178 mm, it is expected that a future experiment would demonstrate a slightly higher increase in intensity if the experiment was repeated at the same distance in both cases.

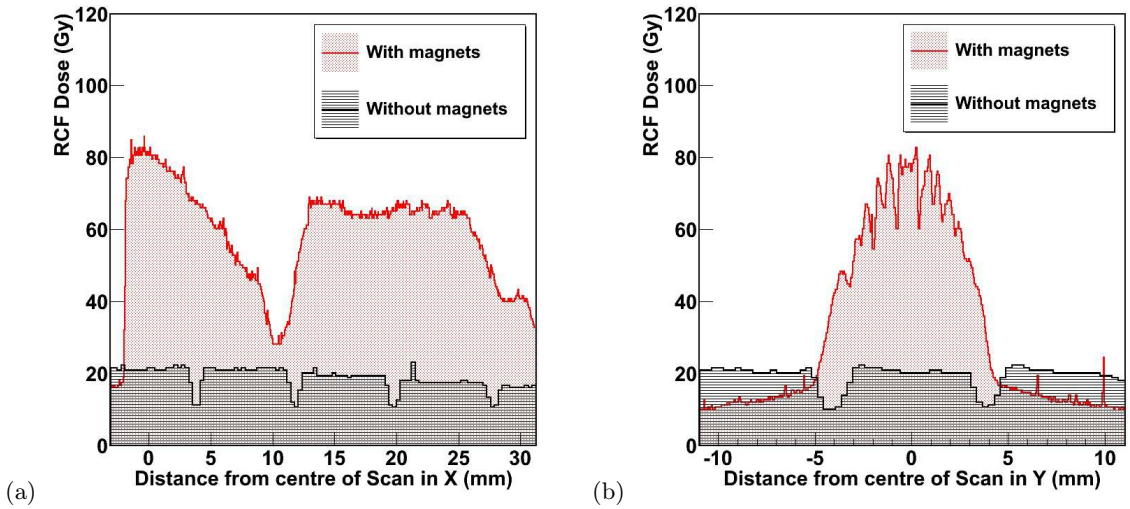

Figure 21: Analysis of the dose measured in the RCFs shown in Fig 20(a) and (b). Note that the orientation of Fig 20(b) was rotated 180° for the purpose of this analysis since a re-scan was required to analyse the dose. A profile analysis is done in the horizontal direction (a) and vertical direction (b). Red shows data obtained using the PMQ triplet, and Black shows data obtained with no magnets in the beamline.

Fig 22 shows an analysis done in GEANT4 of the proton distribution at 442mm behind the scatter foil, with no PMQ triplet in place and at 620mm behind the scatter foil with the PMQ triplet in place. The intensity of the proton beam, as expected, increases dramatically in the focus plane, with up to a four-fold increase in radiation per unit area in the vertical plane, which agrees closely with the real data in Fig 21.

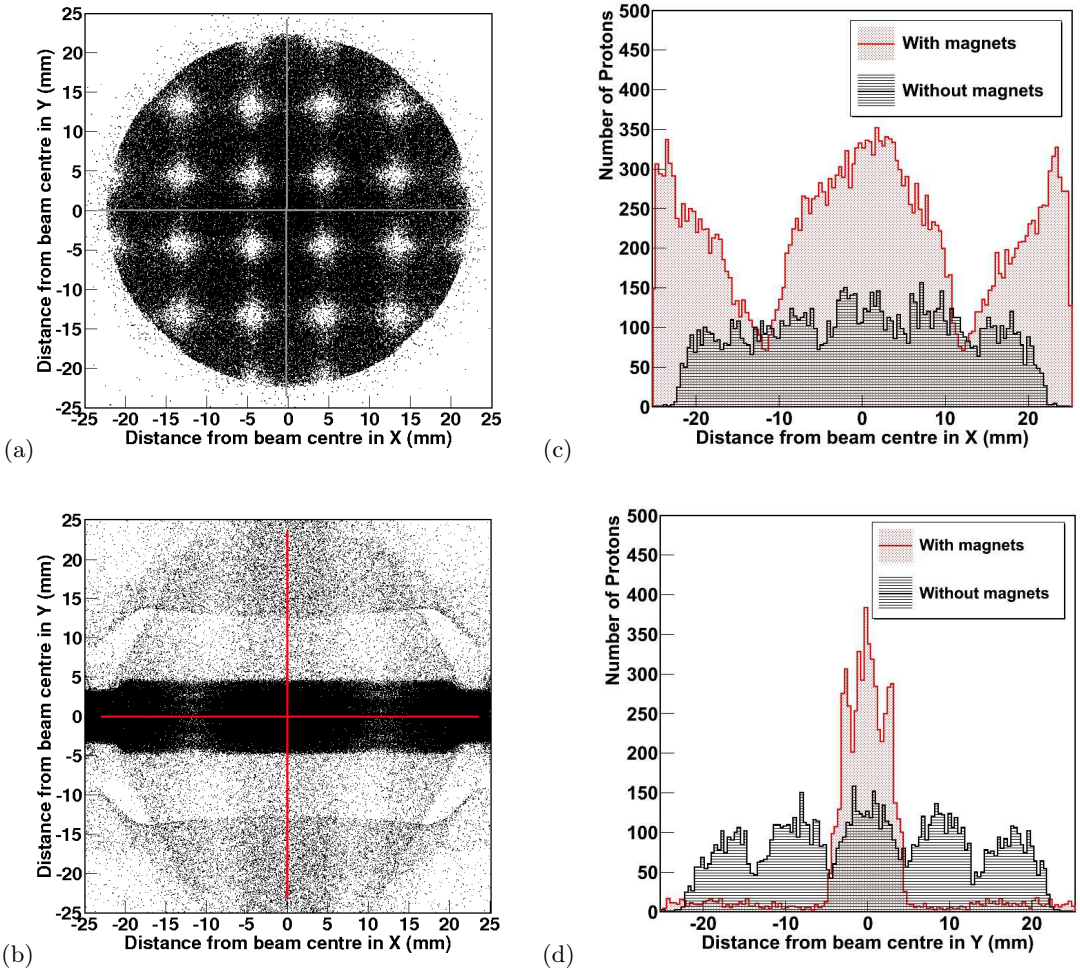

Figure 22: A projection analysis in GEANT4 can quantify the degree to which the beamlets are focussed in a single plane, and the changes in angular acceptance become clear. Comparing between the simulated data with and without the PMQ triplet in place, the analysis is shown for the horizontal plane in (c), and the same analysis performed in the vertical plane is shown in (d). The vertical and horizontal lines on (a) and (b) indicate the position of the analysis. In all of the above the simulation results obtained with the PMQs in place are shaded red, and the equivalent results with no PMQS are shaded black.

The relative intensities predicted by GEANT4, with and without the PMQs present, are in agreement with those seen in the experimental data. One clearly visible effect not accounted for in the simulation is the overlapping of pepperpot beamlets on the RCF film which can be seen clearly in Fig 15(b), which could be due to the far greater number of protons produced during each experimental run than it is possible to simulate in a reasonable time frame with small-scale computational resources. It is expected that this discrepancy could be reduced to some extent by greatly increasing the computational time used for the GEANT4 simulations.

V. CONCLUSION

The methods described in this paper adequately demonstrate the focussing characteristics of a Permanent Magnetic Quadrupole system for both a pencil beam and a diverging beam, and clearly show that such a system will be very useful for a compact proton/ion transport and focussing apparatus. With the advent of new facilities producing laser-accelerated beams of protons and ions, such techniques will be of immense importance for control and optimisation of these beams for physics and medical applications. It is envisaged that advancements on this method, especially increasing the strength and number of the PMQs, will allow new avenues of research in nuclear and plasma physics of astrophysical relevance. When coupled with dipoles to disperse proton energies this technology can also be used to provide mono-energetic beams from the broad energy range of beams typically seen with laser produced protons.

Using the studies and simulation techniques presented here, we hope to use these techniques on a laser system to demonstrate the inherent benefits that focussing, control and transport of a laser-produced proton beam have in comparison with current accelerator technology.

---

[1] K.W.D.Ledingham and P.J.Norreys. *Contemp. Phys.*, 40:367, 1999.
[2] T.Hideaki. *J. Plasma and Fusion Research*, 77:1097, 2001.
[3] K.W.D.Ledingham, P.McKenna, and R.P.Singhal. *Science*, 300:1107, 2003.
[4] K.W.D.Ledingham and W.Galster. *New J. Phys.*, 12, 2010.
[5] H.Schwoerer et al. *Nature*, 439:445, 2006.
[6] B.M.Hegelich et al. *Nature*, 439:441, 2006.
[7] T.Toncian et al. *Science*, 312:410, 2006.
[8] U.Linz and J.Alonso. *Phys.Rev.ST Accel.Beams*, 10(094801), 2007.
[9] R.Coehoorn et al. *Journal De Physique*, C8:669, 1988.
[10] K.Halbach. *Nucl. Instrum. Methods*, 187:109, 1981.
[11] S.M.Wiggins et al. *Plasma Phys. Control. Fusion*, 52(124032), 2010.
[12] J.K.Lim et al. *Phys.Rev.ST Accel.Beams*, 8(072401), 2005.
[13] T.Eichner et al. *Phys.Rev.ST Accel.Beams*, 10(082401), 2007.
[14] H.Chen et al. *Rev. Sci. Instr.*, 79(10E533), 2008.
[15] M.Schollmeier et al. *Phys.Rev.Let.*, 101(055004), 2008.
[16] S.Becker et al. *Phys.Rev.ST. Accel.Beams.*, 12(102801), 2009.
[17] J.Mallinson. *IEEE Transactions on Magnetics*, 9(4):678, 1973.
[18] H.A.Enge. *Rev.Sci.Instrum.*, 30:248, 1959.
[19] M.Friedrich, W.Bürger, R.Grötzschel, D.Henke, G.Sun, D.Herbert, T.Rothe, and W.Stolz. *Nucl. Instrum. Methods*, B 92(1-4):58, 1994.
[20] H.Wiedemann. *Particle Accelerator Physics*, chapter 2.2, page 45. Springer, 2nd edition, 1999.
[21] TOSCA. Magnetostatic field analysis. *OPERA-3D User Guide*, 2008. Vector Fields, 24 Bankside, Kidlington, Oxford OX5 1JE, UK.
[22] X.Zhu et al. *Applied Surface Science*, 152(3):138, 1999.
[23] P.J.Scully, D.Jones, and D.A.Jarozynski. *J.Opt.A: Pure Appl. Opt.*, 5:S92–S96, 2003.
[24] S.Agostinelli et al. *Nucl. Instrum. Methods*, A 506:250, 2003.
[25] J.C.Butcher. The numerical analysis of ordinary differential equations: Runge-Kutta and general linear methods. *Wiley-Interscience*, 1987.
[26] M.R.Mitchell. Private communication.
[27] R.Brun and F.Rademaker. ROOT - an object oriented data analysis framework. *Nucl. Inst and Meth. in Phys. Res.*, A(389):81–86, 1997.